Proceedings World Geothermal Congress 2026
Calgary, Canada, June 8 – 11, 2026

Electric Self-Potential Monitoring of Hydraulic Fracturing

E. Schill*, N. Nakata, E. Um, M. Wilt, E. Nichols, T. Wood and A. Nayak
Lawrence Berkeley National Laboratory
eschill@lbl.gov*

Keywords: Electric self-potential, hydraulic fracturing, lab-to-field scale

INTRODUCTION

Fracture creation and the enhancement of natural fracture volume are key processes in Enhanced Geothermal Systems (EGS). EGS are typically developed in low-permeability, often granitic basement rocks to enable geothermal heat and power production independent of naturally occurring hydrothermal reservoirs. Throughout the evolution of EGS development, hydraulic fracturing and shearing techniques have advanced significantly from initial stimulation successes enabling fluid circulation of only a few liters per second (Pettitt, 1981) to rates exceeding 100 L/s and from conventional stepwise injection to cyclic and zipper injection approaches (Schill et al., 2017; Hofmann et al., 2019, 2021; Horne et al., 2025). Most recently, hydraulic fracturing methods have been successfully adapted and implemented around the Utah FORGE site, achieving near-commercial applications, for example at the Cape Station project (McLennan et al., 2023; Horne et al., 2025).

Imaging hydraulic fracturing or shearing and related flow in deep, fractured reservoirs remains a major challenge for geophysical methods. Monitoring induced seismicity provides important insights into the processes of reservoir creation and enhancement but only captures part of the overall response. Significant progress has recently been achieved by combining active-source techniques with distributed acoustic sensing, which allows the detection of fracture opening and closure processes and the identification of potential pre-activation of fractures caused by hydraulic connectivity with preexisting fracture networks (Correa et al., 2024).

Self-potential (SP) has a long history as a valuable geophysical method for geothermal exploration, primarily because of its sensitivity to subsurface fluid flow and its relatively low cost of data acquisition (Corwin and Hoover, 1979). This sensitivity stems from the coupling between fluid flow and electrical potential, described by the electrokinetic coupling coefficient. In essence, when fluids move through the subsurface, they generate an associated electrical field that can be measured at the surface. These measurements can provide diagnostic information about the depth, geometry, and intensity of the pressure and flow sources driving the system.

During hydraulic fracturing, when fluid is injected into newly formed fractures, SP signals are expected to develop in response to the evolving flow field. The temporal and spatial evolution of these signals generally tracks fluid movement and can reveal insights into fracture propagation and connectivity. Because the SP response depends on the rate and volume of injected fluid as well as the geometry of the induced fractures, it can serve as a powerful diagnostic tool for monitoring fracture dynamics and reservoir stimulation in enhanced geothermal systems.

In addition to acoustic/seismic effects, fluid flow also influences the distribution of electric charge carriers (Revil and Jardani, 2013), leading to measurable changes in electrical conductivity. Magnetotelluric and SP methods have been successfully applied during hydraulic reservoir stimulation in several EGS projects worldwide. Changes in electric conductivity and SP have been monitored during experiments with conventional stepwise injection involving predominantly hydraulic shearing at the Soultz site (Marquis et al., 2002; Darnet et al., 2004, 2006), as well as at the Paralana and Habanero projects (Peacock et al., 2012, 2013; Rosas-Carbajal et al., 2015; Didana et al., 2017). Low-volume injection and circulation tests at the Rittershoffen project (Abdelfettah et al., 2018) reveal differences in the electric conductivity response related to injection or production and large fluid losses during drilling the IDDP-2 well were successfully detected by Haaf and Schill (2021).

Overall, two main observations were made:

1) Fluid injection into the reservoir is associated with a decrease in electrical resistivity, as observed during magnetotelluric monitoring.
2) Electric SP increases both, during fluid injection and during pressure shut-in.

This study presents new SP data acquired over approximately one month (August 22–September 19, 2025) at 25 stations during the GOLD hydraulic stimulation at the Cape Modern site in Utah in conjunction with induced seismicity. The relationship between SP variations and seismicity is analyzed to explore the potential for SP data correction. These field-scale observations are compared with a controlled underground experiment conducted at the Äspö Hard Rock Laboratory (HRL; Haaf et al., subm.), where a fracture was generated through a single-step hydraulic injection and subsequently extended by four re-fracturing stages. In the HRL experiment, SP data were recorded at depths of 410 m and 280 m, enabling a detailed comparison between fluid injection and SP.

1 GEOLOGICAL SETTING

The Utah FORGE field laboratory and the Cape Modern EGS project are located near Milford (UT) sitting at the tectonic boundary between the Basin and Range Province and the western margin of the Colorado Plateau. The EGS subsurface target comprises crystalline plutonic basement rocks, primarily granitic intrusions emplaced between 26 and 8 Ma, overlain by volcanic and sedimentary basin-fill units (Moore et al., 2018; Allis et al., 2016). The regional structure dips gently westward beneath the basin, and extensional faulting controls both stress orientation and local fluid pathways (Podgorney et al., 2019). The area is characterized by high heat flow, with temperatures exceeding 200 °C at depths below 3 km (Moore et al., 2020).

2 EXPERIMENTAL SETUP

The experiment was conducted using 29 non-polarizable copper–copper sulfate electrodes filled with NaCl and buried 10 cm below the ground, arranged in two separate electrode chains (Figure 1). These are referred to as the GOLD and FORGE chains, as each includes one electrode positioned near the wellheads at the respective GOLD and FORGE drill pads. The GOLD chain consisted of 18 sensors installed approximately parallel to the horizontal section of the stimulated wells, with four additional sensors aligned in a SSW direction across them. At FORGE, 11 sensors were deployed between the three drill pads along an ESE-oriented profile. Electrode pair spacings and distances to the reference electrode ranged from 200–800 m and 200–1,800 m at GOLD, and from 20–200 m and 200–1,185 m at FORGE.

Data were collected continuously over a one-month period at a sampling frequency of 100 Hz. The monitoring campaign encompassed three distinct phases: approximately one week of baseline measurements prior to hydraulic fracturing, two weeks during which multiple fracturing stages and related events took place, and a final week of post-stimulation monitoring to capture the system's recovery and background conditions.

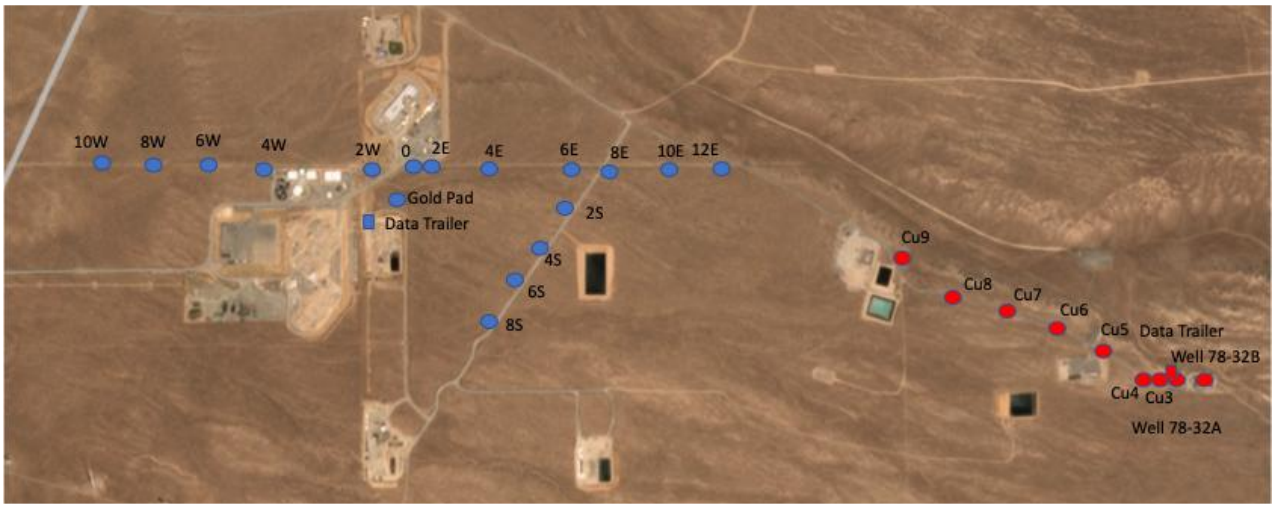


Figure 1. Sensor layout of the FORGE and GOLD electrode chains.

3 FIRST SP MONITORING RESULTS

Our initial analysis of these data consists of examining the time series from individual electrode pairs at varying sampling frequencies. The primary objectives at this stage are to identify correlations between the recorded signals and the observed hydraulic fracturing activity, to characterize the background noise levels, and to develop a systematic plan for subsequent, more detailed data processing and interpretation.

Figure 2 compares the measured SP time series obtained using reference electrodes Cu9 for the FORGE chain (channels 1–9) and 8E for the GOLD chain (channels 10–25) with the sequence of hydraulic fracturing stages in the GOLD wells Gold-4-PB and Gold-8-PB. Hydraulic fracturing began on August 27, 2025, in well Gold-4-PB and

continued in an alternating (zipper) sequence between the two wells. Prior to stimulation, a circulation test was conducted at the Utah FORGE site from August 18–24, 2025.

Figure 3 shows the distribution of automatically picked induced seismic events during the monitoring period. Active vibro-seismic surveys were conducted both before and after the hydraulic fracturing operation, with signals generated by the vibrators shown in the blue areas. These vibro-seismic signals are expected to have influenced the SP recordings.

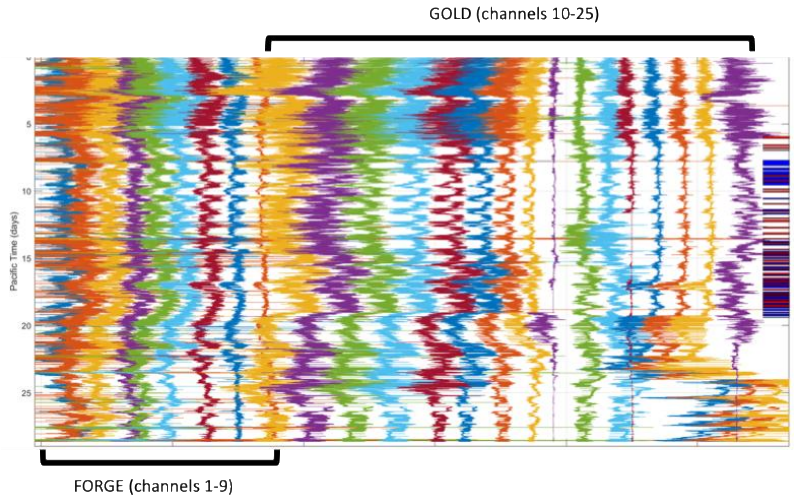


Figure 2. SP time series acquired between Aug 22 and Sept 19, 2025, compared to the fracturing stages in the wells Gold 4-PB (red) and Gold 8-PB (blue) on the right-most column.

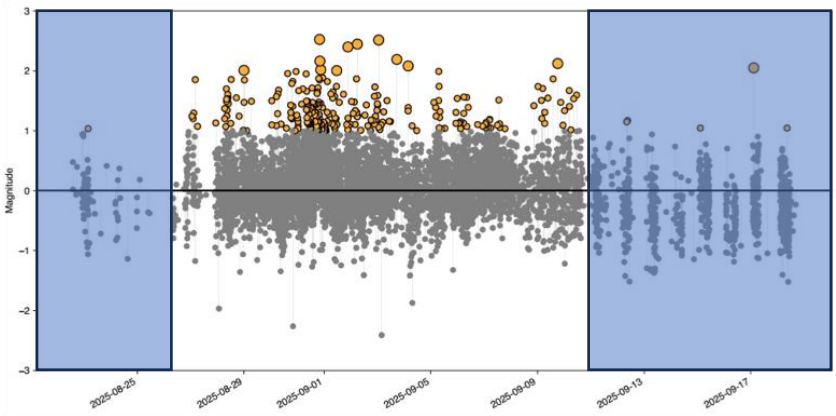


Figure 3. Automatically picked induced seismic events during hydraulic fracturing of the Gold 4-PB and Gold 8-PB wells acquired between Aug 22 and Sept 19, 2025. In the blue area automatic picking reveals signals from the vibro-seismic survey.

The measured SP time series exhibit high-frequency variations with large amplitudes. At the onset of zipper-mode hydraulic fracturing, the SP amplitudes decrease across most channels, with the exception of channels 19 and 20, which show a different response. The amplitudes gradually recover in the GOLD channels that are oriented sub-perpendicular to the stimulated wells, particularly after September 10, 2025, marking the end of the fracturing operations. West of the reference electrode 8E, amplitude recovery occurs earlier, around August 28, 2025, coinciding with a decline in both the number and magnitude of induced seismic events. Notably, automatically detected vibro-seis related signals after September 9, 2025, coincide with distinct variations in the SP recordings. This temporal correlation suggests the potential to identify and correct SP data for anthropogenic noise, an aspect that will be further addressed in the final version of the paper.

4 COMPARISON WITH SP MONITORING OF SINGLE HYDRAULIC FRACTURE

Analogue hydraulic fracturing experiments were conducted in the Äspö HRL (Zang et al., 2017). The tests were performed in the sub-horizontal injection borehole that is sub-parallel (N41°E) to the local minimum horizontal stress direction (Sh). The so-called HF2 experiment took place at a depth of 22.5 m from the TASN wall, reaching a breakdown pressure of 10.91 MPa at a flow rate of approximately 2 L/min, followed by several re-fracturing

stages. After each injection, the borehole was shut-in for 4–5 minutes, then the pressure was released, and the fluid recovered during the bleed-off phase.

In this experiment, the background SP values varied between 0 and <50 mV at short distances and 25–200 mV at several hundred meters from the borehole (Haaf et al., subm.). During the experiment, SP amplitudes ranged from −280 to 610 mV near the borehole and −400 to 200 mV at greater distances. The SP signal increased concurrently with the onset of the first shut-in phase, reaching a maximum of 610 mV about 30 minutes after the main fracturing event. At larger distances, SP changes began slightly later, typically when pressure was released. Following the final re-fracturing stage, a perturbed background level was re-established after approximately 40 minutes.

Key insights from the Äspö HRL experiments that are directly relevant to the GOLD hydraulic fracturing operation include:

1) SP signals at greater distances exhibit temporal delays,
2) SP anomalies from successive fracturing stages overlap, and
3) The SP perturbations influence a relatively large rock volume (Haaf et al., subm.).

The early fracturing stages at GOLD display SP anomalies that are comparable to those observed at Äspö HRL (Figure 4).

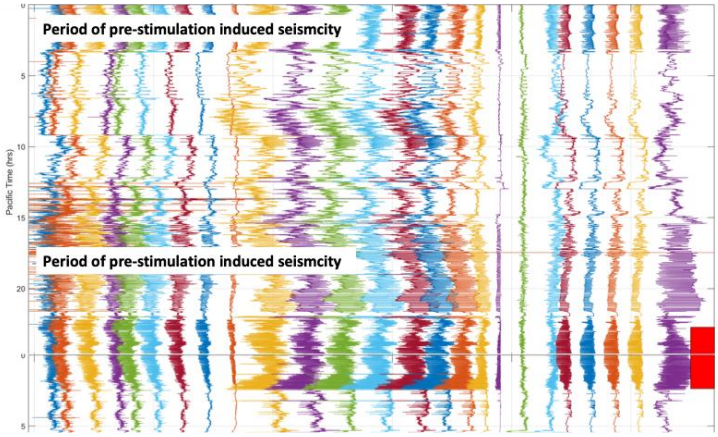


Figure 4. SP time series acquired between Aug 27-28, 2025, compared to the fracturing stage 1 in the Gold 4-PB well (red).

5 FIRST CONCLUSION AND OUTLOOK

Initial analyses of the SP data reveal a clear response to the onset of zipper-style hydraulic fracturing, with a pronounced decrease in SP signal amplitude observed across most channels. This amplitude reduction appears to coincide temporally with key phases of the stimulation, suggesting a possible coupling between fluid injection, subsurface pressure redistribution, and electrokinetic effects. Moreover, the SP time series display temporal correspondence with seismic observations, including both induced seismicity related to hydraulic fracturing and perturbations caused by active vibro-seismic surveys conducted in the same period. Future work will focus on refining the SP dataset through correction procedures that incorporate active seismic signals as a reference for filtering out man-made noise. Once corrected, the SP data will be analyzed in greater detail to isolate the electrokinetic response specifically attributable to fluid injection, fracture propagation, and pore pressure diffusion. This will help to better understand the dynamic coupling between hydraulic, mechanical, and electrical processes during stimulation and evaluate the potential of SP monitoring as a real-time diagnostic tool in EGS operations.

Acknowledgements

We acknowledge the support by the U.S. Department of Energy, Office of Energy Efficiency and Renewable Energy (EERE), Geothermal Technologies Office, under Award Number DE-AC02–05CH11231 with Lawrence Berkeley National Laboratory.

REFERENCES

Abdelfettah, Y., Sailhac, P., Larnier, H., Matthey, P.D. and Schill, E.: Continuous and time-lapse magnetotelluric monitoring of low volume injection at Rittershoffen geothermal project, northern Alsace–France. *Geothermics*, **71**, (2018), 1-11.

Allis, R., Moore, J. N., and Davatzes, N.: The evolving thermal regime at the Roosevelt Hot Springs geothermal system, Utah. *Geothermics*, **64**, (2016), 440–450.

Correa, J., Glubokovskikh, S., Nayak, A., Luo, L., Wood, T., Zhu, X., Ajo-Franklin, J. and Freifeld, B.: Revealing complex subsurface dynamics with continuous seismic monitoring: Observations using distributed acoustic sensing and surface orbital vibrators during hydraulic fracturing. *Geophysics*, **89(6)**, (2024), P47-P56.

Corwin, R.F. and Hoover, D.B.: The self-potential method in geothermal exploration. *Geophysics*, **44(2)**, (1979), 226-245.

Darnet, M., Maineult, A. and Marquis, G.: On the origins of self ‐ potential (SP) anomalies induced by water injections into geothermal reservoirs. *Geophysical Research Letters*, **31(19)**, (2004).

Didana, Y.L., Heinson, G., Thiel, S., Krieger, L.: Magnetotelluric monitoring of permeability enhancement at enhanced geothermal system project. *Geothermics*, **66**, (2017), 23–38.

Haaf, N. and Schill, E.: "Noise" during long-term continuous magnetotelluric monitoring of RN-15/IDDP-2 well engineering (Reykjanes peninsular, Iceland): A geogenic origin?. *Geothermics*, **96**, (2021), 102192.

Haaf, N., Jougnot, D., Guarracino, L., Niemz, P., and Schill, E.: Electric self-potential monitoring of hydraulic fracturing in the Äspö Hard Rock Laboratory, Sweden. *Geothermics*, (subm.)

Hofmann, H., Zimmermann, G., Farkas, M., Huenges, E., Zang, A., Leonhardt, M., Kwiatek, G., Martinez-Garzon, P., Bohnhoff, M., Ki-Bok Min, Fokker, P., Westaway, R., Bethmann, F., Meier, P., Kern Shin Yoon, Jai Won Choi, Tae Jong Lee, and Kwang Yeom Kim: First field application of cyclic soft stimulation at the Pohang Enhanced Geothermal System site in Korea. *Geophysical Journal International*, **217**, (2019), 926–949.

Hofmann, H., Zimmermann, G., Huenges, E., Regenspurg, S., Aldaz, S., Milkereit, C., Heimann, S., Dahm, T., Zang, A., Grigoli, F., Karvounis, D., Briccardo, M., Wiemer, S., Hjörleifsdóttir, V., Kristjánsson, B.R., Hersir, G.P., Ásgeirsdóttir, R.S., Magnússon, and R., Árnadóttir, S.: Soft stimulation treatment of geothermal well RV-43 to meet the growing heat demand of Reykjavik. *Geothermics*, **96**, (2021).

Horne, R., Genter, A., McClure, M., Ellsworth, W., Norbeck, J. and Schill, E.: Enhanced geothermal systems for clean firm energy generation. *Nature Reviews Clean Technology*, **1(2)**, (2025), 148-160.

Marquis, G., Darnet, M., Sailhac, P., Singh, A.K. and Gérard, A.: Surface electric variations induced by deep hydraulic stimulation: An example from the Soultz HDR site. *Geophysical Research Letters*, **29(14)**, (2002), 7-1.

McLennan, J., England, K., Rose, P., Moore, J., and Barker, B., 2023, January. Stimulation of a high-temperature granitic reservoir at the Utah FORGE site. SPE hydraulic fracturing technology conference and exhibition

Moore, J. N., Simmons, S. F., Podgorney, R.: The Utah FORGE site: An EGS laboratory in the Basin and Range transition zone. *Geothermal Resources Council Transactions*, **42**, (2018), 503–516.

Moore, J. N., et al. (2020). Geologic setting and evolution of the Utah FORGE site. *Geothermal Resources Council Transactions*, **44**, 1151–1164.

Peacock, J.R., Thiel, S., Reid, P. and Heinson, G.: Magnetotelluric monitoring of a fluid injection: Example from an enhanced geothermal system. *Geophysical Research Letters*, **39(18)**, (2012).

Peacock, J.R., Thiel, S., Heinson, G.S. and Reid, P.: Time-lapse magnetotelluric monitoring of an enhanced geothermal system. *Geophysics*, **78(3)**, (2013), B121-B130.

Pettitt, R.A.: Development of man-made geothermal reservoirs. Report, No. LA-UR-81-852; CONF-810808-4. Los Alamos National Lab., NM, USA (1981).

Podgorney, R., McLennan, J., Moore, J. N., and Allis, R.: Utah FORGE: A path toward large-scale EGS demonstration. *Proceedings*, 44th Workshop on Geothermal Reservoir Engineering, Stanford University, (2019)

Rosas-Carbajal, M., Linde, N., Peacock, J., Zyserman, F.I., Kalscheuer, T. and Thiel, S.: Probabilistic 3-D time-lapse inversion of magnetotelluric data: application to an enhanced geothermal system. *Geophysical Supplements to the Monthly Notices of the Royal Astronomical Society*, **203(3)**, (2015), 1946-1960.

Schill, E., Genter, A., Cuenot, N., and Kohl, T.: Hydraulic performance history at the Soultz EGS reservoirs from stimulation and long-term circulation tests. *Geothermics*, **70**, (2018), 110–124.